DISLOCATION ARRANGEMENT IN COPPER SINGLE CRYSTALS DEFORMED AT LOW TEMPERATURES

Z. S. Basinski
National Research Council, Ottawa, Canada

The phenomenon of the plastic deformation of crystals, and, in particular, the aspect of work hardening, presents a very complex problem. To understand it we must explain the macroscopic observations, such as the stress strain curve with its dependence on temperature, strain rate, crystal orientation and impurity content, and also account for the various microscopic features such as the development of particular substructure, surface observations, etc. This would apply even if we are trying to explain the behaviour only of a particular crystal type, e.g., f.c.c.

In recent years, direct observation of thin sections of deformed crystals by transmission electron microscopy has been added to the already large arsenal of methods used in the study of plastic deformation, and, for a while, it appeared that the problem was almost solved. However, it now seems that the additional data only show that the process is much more complex than had been envisaged. The existing explanations of the work hardening process fall into several groups based on different structural models, and it should be possible to assess the validity of these on the basis of experimental observations. However, very often the experimental observations are inconclusive and critical experiments, for many reasons, are lacking.

Thin foil techniques suffer from the danger that the observed dislocation distribution may not be representative of the bulk material. Slip line measurements, on the other hand, are made on the surface region which may be atypical. Macroscopic deformation behaviour can be influenced by even minute amounts of impurity. It therefore seems advisable to collect as much information as possible and assess it carefully.

The present work deals with the deformation behaviour of Cu single crystals as studied by a combination of slip line observations, etch pit techniques and transmission electron microscopy. Copper crystals of preselected orientations were grown from the melt in graphite molds. The copper used was 99.999%, from American Smelting and Refining Company. To reduce the number of possible variables, the stress strain curve was obtained at low temperatures (usually 4.2°K), the effect of diffusion during deformation could then be neglected. Since warming copper specimens to room temperature for subsequent study did not affect either the flow stress or rate of strain hardening (Blewitt et al, 1957), subsequent changes are therefore not considered to be of major importance. After deformation the crystal was sliced to desired

orientations using a Servomet spark cutter modified to give a spark energy of about 1 erg per spark. The temperature rise 1/10 mm from the face being cut was less than 15°C, and the spark damage determined by dislocation etch pit counts on well annealed crystals was confined to a depth of less than 1/10 mm. Specimens were prepared from the slices by the method of Wilsdorf et al (1958) and examined in a Siemens Elmiscope I operating at 100 K.V. Specimens were examined in various reflections to determine the Burgers vectors of the dislocations present. The relative distribution of dislocations in three dimensions was determined by preparing stereo-photographs, (Basinski, 1962), using a Valdré goniometer stage (1962).

Etch Pit Measurements

The variation of dislocation density and distribution was studied by various authors, (e.g. Livingston, 1962; Young, 1961; Hordon, 1962). Livingston's data show that the flow stress correlates quite well with dislocation density except in the early stages of deformation of crystals oriented for single glide, where the etch pit density is somewhat high.

The orientation of the crystals used in the present work was almost identical with the single glide crystals of Livingston, the tension axis lay 8° away from the <110> direction on the great circle between the corner of the standard triangle and the slip direction. Etch pits were examined both on the cross glide plane and on the main glide plane to examine the difference between dislocation density lying in and threading the primary glide plane.

Fig. 1 shows the plot of the etch pit density versus flow stress. Livingston's data are included for comparison. In general the forest density is somewhat lower than the dislocation density lying in the main glide system; this difference decreases at higher stresses. No sign of a systematic deviation in the flow stress-density relation occurs for the forest dislocations although it is desirable to check this point further by making more measurements at lower stresses. The distribution of the etch pits on the cross and main glide planes is markedly different. Those on the cross glide plane are nonuniformly distributed and show alignment along the traces of the main glide plane, glide polygonisation, and an increase in etch pit density near sub-grain boundaries. These observations are in agreement with Livingston's work. The distribution of etch pits on the main glide plane, on the other hand, is much more uniform, no increase in etch pit density near sub-boundaries is observed (Fig. 2).

The absence of an increase in etch pit density near the sub-boundaries on the main glide plane indicates that dislocations of the secondary system move a distance short in comparison with the mean sub-grain size, and in spite of their comparatively large number presumably do not contribute appreciably to the overall

strain. This would appear to remove an important difficulty facing the observations, arising from the fact that the lattice rotations produced during deformation are well accounted for by assuming deformation on the primary system only, (e.g. Ahlers and Haasen, 1962), especially since the X-ray measurements would be insensitive to small amounts of strain occurring on other systems.

Further evidence for the activity of slip systems other than the primary one, even in the early stages of deformation, can be obtained from slip line observations. Fig. 3 shows slip lines on the cross slip plane of a specimen deformed to $345 g/mm^2$. Since the slip direction here lies in the plane of observation the primary system cannot produce any visible surface changes.

Foil Observations

Specimens deformed in easy glide show mainly edge dislocations belonging to the primary glide system. These, as expected from etch pit data, are distributed extremely unevenly with large areas of the foil being completely free of dislocations. Fig. 4 shows a region having a high density of dislocations. The primary glide direction here is vertical, and the dislocations have a form strongly resembling the "dipoles" observed in fatigued specimens (e.g., Segall, 1959), and in specimens deformed in tension, (e.g. Wilsdorf and Wilsdorf, 1961). On closer examination it is apparent that these are arranged in dense walls which contain not only dipoles but also single edge dislocations.

Occasionally the dislocation-free regions on either side of the wall have different contrast resulting from an excess of one sign of Burgers vector causing lattice tilting; but in most cases no difference in contrast is observed, indicating that the Burgers vectors of the dislocations in the wall add approximately to zero.

Another type of defect visible at this stage are straight faint segments of dislocation which end within the crystal. These invariably run along two of the $<110>$ directions lying in the slip plane other than the slip direction. They have been shown (Howie, 1962) to be very narrow dipoles bounded by Frank sessile dislocations.

A very characteristic feature recurring in most of these photographs is the coincidence of dipole ends and other features along certain cross slip planes. The imperfect alignment of these ends in the two dimensional photographs can be seen in three dimensions to be due to the different depth of dipoles in the foil. These "slicing planes" are indicated by arrows in Fig. 4. Long dipoles must therefore have been cut into shorter pieces by slip occurring on cross slip planes. Since there is no evidence left at the ends of cut dipoles of trails which would indicate distributed slip, relatively large amounts of slip must have occurred on isolated or very closely spaced planes. The direction of this slip must have

had at least a component normal to the glide plane to account for the cutting of the dipoles, and displacing single dislocations into planes above or below their original plane (e.g. A in Fig. 4).

The dense regions of dipoles invariably show complex interactions along such a "slicing plane" (B in Fig. 4) and very often show there dislocations with different Burgers vectors (Fig. 5). These types of interaction can also be clearly seen in Fig. 6 obtained from a specimen strained to 340g/mm^2, and in fact on most photographs at this, and higher strains. This observation strongly suggests that the short dipole loops commonly seen, especially at higher strains, in deformed crystals result from chopping much longer dipoles probably formed originally by the lining up of edge dislocations, and not by repeated cross slip mechanisms (e.g., Johnston and Gilman, 1960) or dislocation interaction mechanisms proposed by Tetelman (1962).

A large number of short dipoles were usually observed in the vicinity of sub-grain boundaries, as can be seen in Fig. 7. The sub-grain boundary was identified by developing etch pits on the specimen after observation in the microscope, the boundary was seen to cross the carbonised region. These dipoles would appear as dense etch pits near a sub-boundary on the cross slip plane, but not on the main glide plane.

Stage II General Features

The following section refers mainly to work carried out with Dr. D. B. Dove, (to be published).

Electron microscopic observations on copper specimens from strip crystals deformed at low temperatures (78°K and 4.2°K) in Stage II show dense dislocation tangles which tend to lie on planes parallel to those for which the resolved shear stress is high. Similar observations were made by Howie (1960) in CuAl alloy crystals deformed at room temperature.

For crystals oriented for single glide most of the tangles are parallel to the primary glide plane, but some do lie on other planes; the frequency with which they occur being approximately in proportion to the resolved shear stress on that particular plane. Fig. 8.

The presence of strong contrast indicates that the dislocations in a tangle cause appreciable lattice rotation across it. This rotation was analysed in the electron microscope by examining the relative displacement of Kikuchi lines resulting from scattering by portions of the crystal on either side of a dense dislocation tangle. In every case examined the rotation axis appeared to lie in the slip plane (i.e. the plane of the tangle) normal to the slip direction. This, in fact corresponds to the rotation axis which is known to occur in the kink bands. Here,

however, the boundary lies in the slip plane and not in the plane normal to it. The displacement of Kikuchi lines gives information on only two components of rotation, the component parallel to the electron beam is difficult to determine, and in order to check this, some slices were cut having normals, (a) in the slip direction, and (b) lying in the main glide plane and perpendicular to the slip direction. Strong contrast across dislocation walls in specimens of the first type, and almost complete absence of such contrast in specimens of the second type, viewed in various reflections, supports the original conclusion.

When the crystals are oriented for double glide the dislocation tangles present a very striking cross-grid pattern (Fig. 9).

There does not seem to be much reliable evidence on the Burgers vectors of dislocations lying in these tangles. One important question is what proportion of the dislccations have Burgers vectors belonging to the primary slip system. Fig. 10 shows a specimen photographed in the reflection of the primary slip plane; all dislocations having Burgers vectors lying in this plane are therefore not visible. It is apparent that there is a very large number of dislocations belonging to systems other than the primary glide system. A striking feature of this figure is that even though the primary glide dislocations are absent, it is very easy to pick out the traces of the primary glide plane. It may be concluded from this feature that a relatively large number of sources on the secondary systems emit a small number of dislocations which travel short distances, rendering the deformation here much more homogeneous, and making its detection by either slip line studies or lattice rotation extremely difficult.

Photographs of specimens obtained from the surface regions of crystals deformed in Stage II show that the dislocation distribution there is quite different from that in the interior of the crystal. Fig. 11 shows part of a foil polished from one side only. Slip lines, due to changes in thickness, are clearly visible. In spite of the close correlation between the prominent directions on the surface and in the interior of the crystal, there is very little correlation between slip lines and the crystal just underneath them. The dislocations here are less tangled and are arranged approximately at random. That the material just under the surface is atypical is hardly surprising since not only are the dislocations near the surface subjected to image forces which may modify their behaviour, but also a large number of dislocations leave the crystal to produce slip bands. Whereas in the interior of the crystal dislocations travel in both directions, unless a large number of additional sources operates at the surface (corresponding to the number contained in a slab whose thickness is equal to the dislocation mean free path), the loss of dislocations at the surface must be compensated by an increase in the distance travelled by the dislocations in this region.

Dislocation Networks in the Main Glide Plane

To attempt to elucidate the nature of the dense dislocation tangles sections of the crystal were cut parallel to the main glide plane, from crystals stretched up to about 1.7kg/mm^2. Several distinct types of dislocation arrangements were to be observed. One feature is the three dimensional networks containing a large number of short segments of Cottrell-Lomer dislocations. These result from reaction at the intersection with both the conjugate and critical slipplanes, however, specific areas usually contain a predominance of one type. Fig. 12a shows a typical example of such a region. In Fig. 12b, the Cottrell-Lomer dislocations are invisible.

In some regions, portions of the crystal which are reasonably free of dislocations are separated by long narrow tangles lying along the traces of the highly stressed secondary slip plane (Fig. 13). These presumably occur when sections are cut between the dense networks of the main glide system, and show a section through a steeply inclined secondary glide tangle. Here a large number of edge dislocation dipoles belonging to the primary glide system is visible, and suggests quite an extensive crossing of these tangles by primary glide dislocations. This is rather similar to the large number of primary glide dislocation dipoles associated with the sub-grain boundary, as in Fig. 7.

In some areas dense patches of short dipoles were observed. As expected the Burgers vectors of the dislocations comprising them always lay in the slip direction.

Preliminary observations on a crystal whose tension axis lay in the $<211>$ direction indicate that the distribution of dislocations here is not fundamentally different from that in crystals oriented for single glide. In this case, however, mainly Cottrell-Lomer dislocations resulting from interaction with the conjugate system were observed. So far, no dense networks were seen in which the Cottrell-Lomer dislocations completely predominate. This may not be significant since the number of specimens of this orientation examined was small.

Sections parallel to both of the active glide planes showed also dipole patches in each case lying in the plane of observation. Here too, as in easy glide of crystals oriented for single slip, the "slicing" on the cross slip plane could clearly be seen. An example is shown in Fig. 14.

Discussion

From the data presented it appears that in copper crystals deformed at low temperatures in Stage I most of the dislocations remaining in the lattice are edge dislocations belonging to the primary slip system. Comparison of the dislocation densities obtained from etch pit data, with the strain, gives for the

dislocation mean free path, $\lambda \simeq \frac{\varepsilon}{\rho b}$, the surprisingly large value of 2-4 mm. This may be compared with a value of about 25μ obtained by Wilsdorf and Schmitz (1962) in aluminium deformed at room temperature. Although the estimate for copper may be somewhat high, since dense clumps of edge dislocations may not be resolvable into individual etch pits, it is improbable that this would account for a difference of a factor of 10^2. It is difficult to estimate the dislocation density in Stage I from thin foils because of the very nonuniform distribution. However, in Stage II the densities from thin foil counts and etch pit counts agree to within a factor of 2. It therefore appears that the discrepancy must lie in a difference in both material and the temperature of deformation. The large mean free path of the dislocations in easy glide is also indicated by the large scale crossing of sub-boundaries. It is not clear at present whether screw dislocations are not visible because they cross slipped during deformation or because they are lost from the foil during thinning.

In spite of the long mean free path, the dislocation density on the primary glide plane is still larger than would be expected from the flow stress. These dislocations therefore cannot harden the crystal very effectively. It is often asserted (Seeger et al, 1961) that the forest density does not increase during easy glide and only slowly even in Stage II. These authors assume that the temperature dependent flow stress comes from the forest contribution and the lack of its increase in easy glide is taken as evidence of no increase in the forest density. Recent work (Basinski and Dove, to be published) has shown, however, that the flow stress ratio in the early stages of deformation is extremely sensitive to small amounts of impurity, and therefore the forest contribution to the temperature dependent flow stress may be completely swamped by the impurity contribution during easy glide.

The present results leave little doubt that the forest density does increase during deformation.

Several mechanisms have been proposed for the formation of dislocation dipoles, sometimes called prismatic loops, during deformation. The first mechanism considered by various authors, (e.g. Johnston and Gilman, 1960; Price, 1960; Wilsdorf and Fourie, 1960) envisages cross slip by a screw dislocation with the formation of a large jog which during subsequent glide gives rise to a dislocation dipole. Cross slip to the original plane then completes the process producing a prismatic dislocation loop. It is difficult to see how a large length of dislocation would cross slip simultaneously; and cross slip by a short segment would produce two dipoles of opposite sign close to each other, which could then easily annihilate by gliding during subsequent deformation. Furthermore, recross-slipping of a screw dislocation to its original plane appears to be a rather improbable process. A more plausible mechanism proposed by Tetelman (1962) envisages an elastic interaction between

dislocations having an edge component and lying on a parallel glide plane, followed by cross slip of the screw components separating a prismatic loop.

The perfect alignment of dipole ends on a particular cross slip plane almost invariably observed, however, supports the view that the mechanism of this loop formation may be much simpler. Edge dislocations mainly during Stage I of the deformation get stopped by other edge dislocations producing reasonably long dislocation walls, which subsequently get cut into shorter pieces by slip on the cross glide plane. A large number of short dipoles could be produced by such a process. Since the long range stresses would favour the formation of edge dislocation tangles composed of dislocations of opposite signs we would expect that dipoles would predominate over single dislocations in such a wall.

With increasing deformation in Stage II the relative prominence of the dipoles decreases rapidly and it is quite probable that not many of them are formed once the other systems become more active, and that the dislocations in Stage II are stopped by other interactions.

Stage II

The most noticeable change in the dislocation arrangements with the onset of Stage II is the increasing appearance of dislocations with Burgers vectors other than that of the main glide system, until, at stresses of about 2 - 3kg/mm^2 the predominance of dislocations of the primary system over any other seems to be almost lost. At first sight this observation may seem rather surprising in view of the fact that most of the strain appears to have been produced by the operation of the primary systems in crystals oriented for single glide. But, unless the slip on the primary system is distributed extremely homogeneously, or the slip displacement continues in each packet right across the crystal, large accommodation stresses will be present which can only be relieved by glide on secondary systems. Reactions between the primary and secondary dislocations then could produce the networks observed in Stage II. The presence of tangles in crystals deformed at liquid helium temperature shows that interaction with point defects (Wilsdorf and Wilsdorf, 1961) is not necessary for their formation.

The lattice rotations observed around the $\langle 211 \rangle$ direction are surprising since it is not easy to see how a simple dislocation network could produce them without involving a prohibitive amount of long range stress. However, Cottrell-Lomer barriers lying in both of the possible directions were observed and it can be shown that a combination of these with some screw dislocations derived from the two other slip directions lying in the primary glide plane could produce a network free of long range stresses and giving the required lattice rotation. It may be that this type of rotation is preferred by

the lattice to the twist type boundary, because it does not require very large additional accommodation at the ends of a cell.

Much additional work, however, especially involving careful analysis of all the components of the dislocation networks is required before all the aspects of deformation mechanisms can be understood.

REFERENCES

Ahlers and Haasen, P. 1962 Acta Met. 10, 977 (L).
Basinski, Z. S. 1962, 5th Int. Cong. Elec. Microscopy, Philadelphia, 1, B13.
Blewitt, T. H., Coltman, R. R. and Redman, J. K. 1957, J. Appl. Phys. 28, 651.
Fourie, J. T. and Wilsdorf, H. G. F. 1960, J. Appl. Phys. 31, 2219.
Hordon, M. J. 1962, Acta Met. 10, 999.
Howie, A. 1960, Ph.D. Thesis (Cambridge) and European Regional Conference on Electron Microscopy, Delft 1960, 383.
Howie, A. 1962, Private communication.
Johnston, W. G. and Gilman, J. J. 1960, J. Appl. Phys. 31, 632.
Livingston. 1962, Acta Met, 229.
Price, P. B. 1960, Phil. Mag. 5, 873.
Seeger, A., Kronmuller, H., Mader, S. and Trauble, H. 1961, Phil. Mag. 6, 639.
Segall, R. L. and Partridge, P. G. 1959, Phil. Mag. 4, 912.
Valdré, U. 1962, J. Sci. Inst. 39, 278.
Wilsdorf, H. G. F., Cinquina, L. and Varker, C. J. 1958, 4th International Conference on Electron Microscopy, Berlin, 559.
Wilsdorf, H. G. F. and Schmitz, J. 1962, J. Appl. Phys. 33, 1750.
Wilsdorf, H. G. F. and Wilsdorf, D. 1961 Proc. 1st Int. Mat. Conf. Berkeley.
Young, F. W. 1961, J. Appl. Phys. 32, 192.

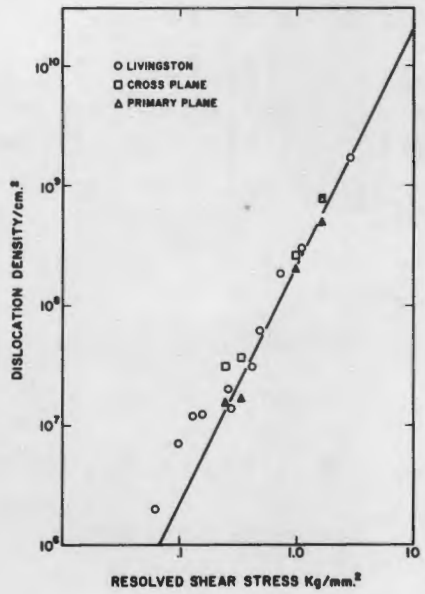

Figure 1 Etch pit density versus stress.

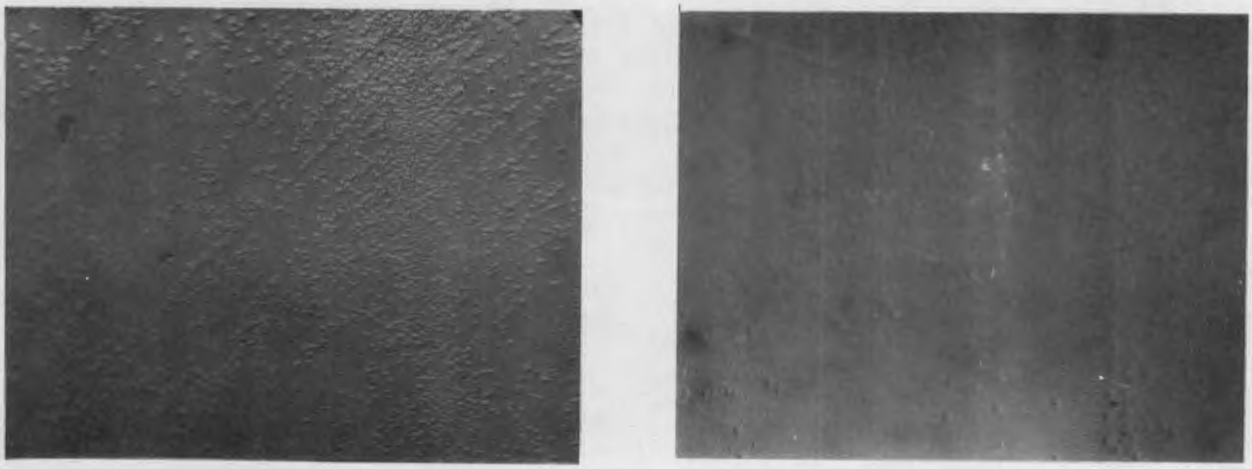

(a) (b)

Figure 2. Dislocation etch pits; (a) cross slip plane; (b) main glide plane, note absence of increased density near sub-boundary.

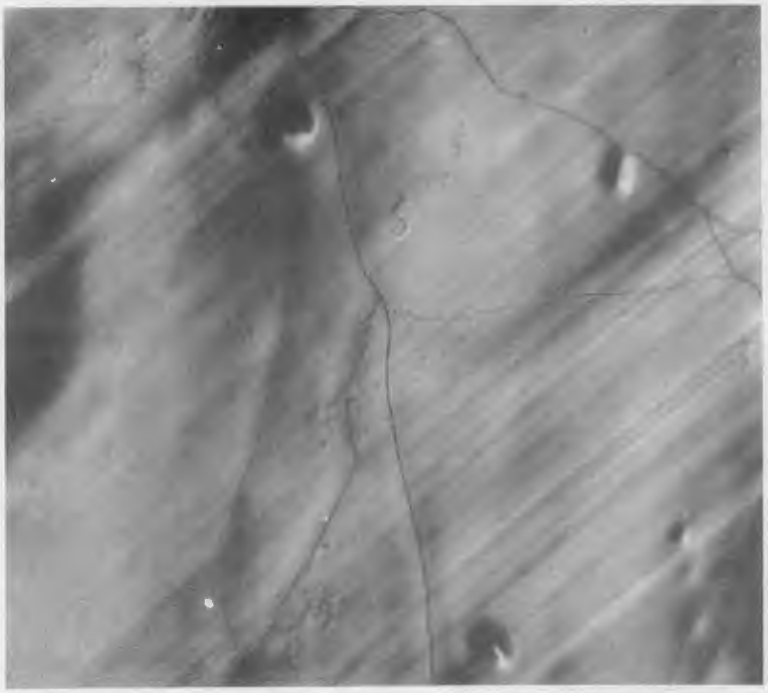

Figure 3. Slip lines on cross slip plane. (x 225). Resolved shear stress 345g/mm^2.

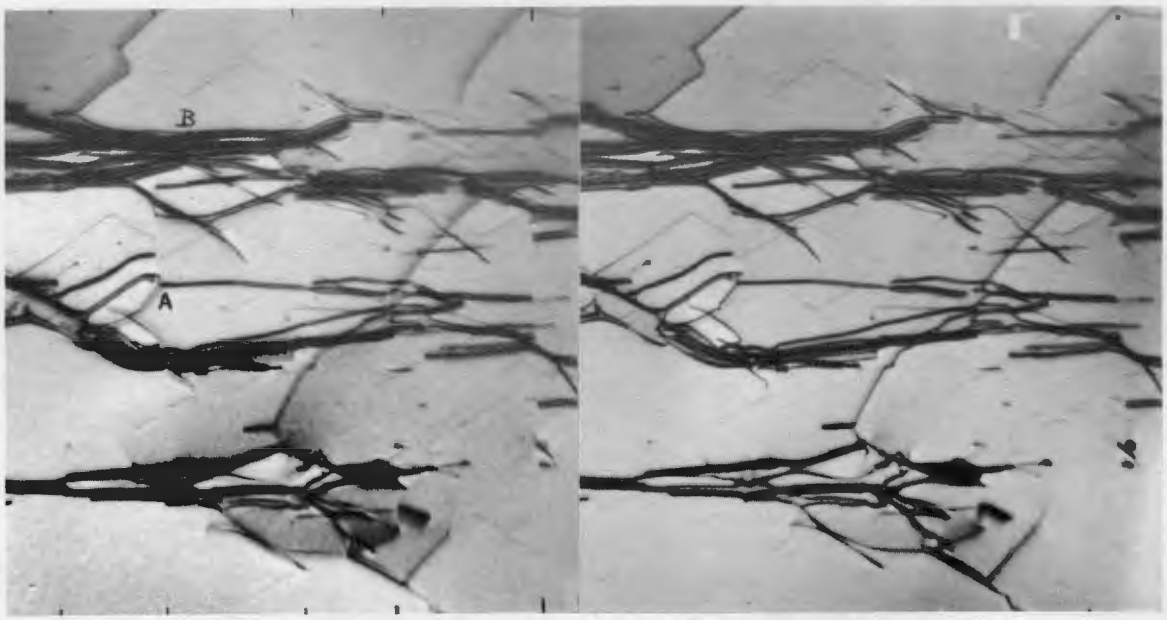

Figure 4. Stereo pair of a dislocation clump in the early stage of deformation. σ = 245g/mm^2., deformed at 4.2 K.. Section parallel to main glide plane. Slip direction vertical. (x 15,000).

Figure 5. Same as 4, g.b = 0 for main glide system.

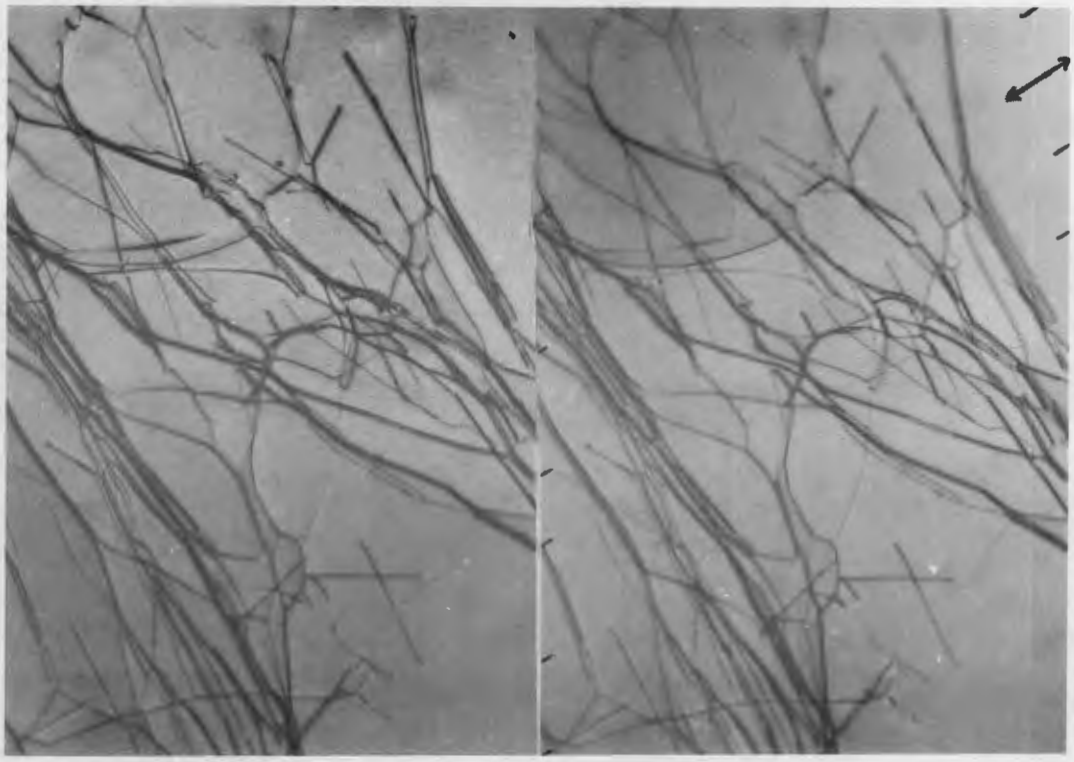

Figure 6. Stereo pair later in easy glide. Section parallel to main glide plane, slip direction indicated by arrow. (x 15,000)

Figure 7. Section showing sub grain boundary. (x 15,000)

Figure 8. Strip crystal deformed at 4.2°K in stage II. Single glide orientation. Not dislocation tangles and contrasts parallel to main glide plane. (x 15,000) (Basinski & Dove, to be published.)

Figure 9 Crystal deformed at 78°K. Double glide orientation. (x 15,000) (Basinski & Dove, to be published.)

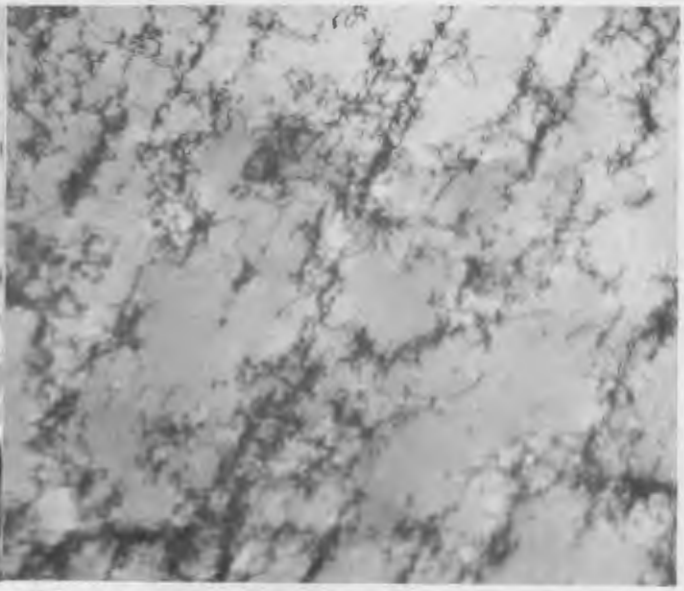

Figure 10. Crystal in single glide orientation, deformed at 4.2°K. Contrast from reflection in main glide plane; dislocations with Burgers vectors lying in this plane are invisible. (15,000) (Basinski & Dove, to be published)

Figure 11. Copper, single glide orientation, deformed at 4.2°K. Polished from one side only. Note the absence of correlation between slip lines and dislocation arrangement. (x 15,000).

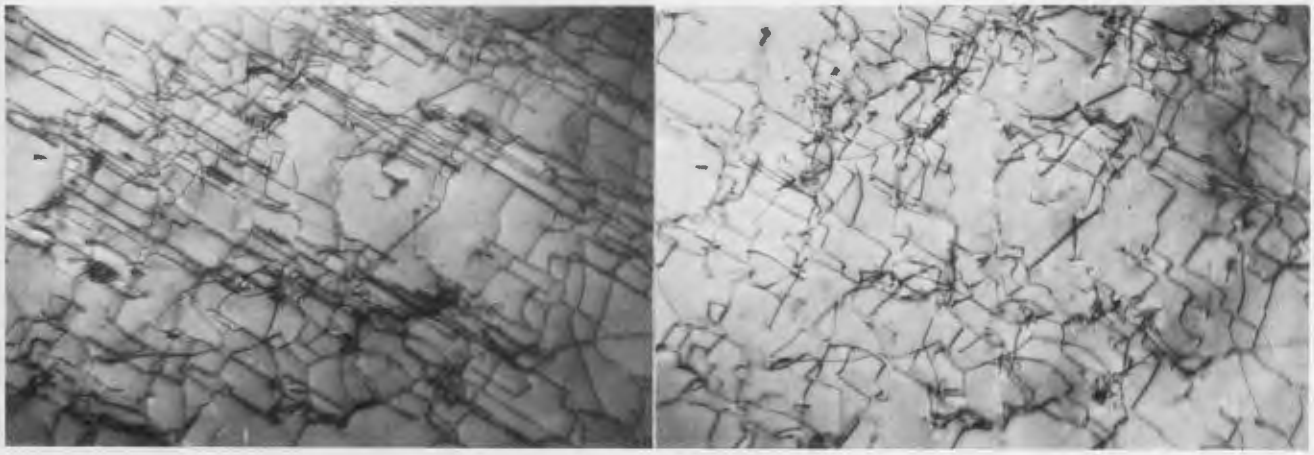

(a) (b)

Figure 12. Network containing a large number of Cottrell-Lomer dislocations. Section parallel to main glide plane. In 12 (b) g.b for Cottrell-Lomer dislocations is zero. σ = 995g/mm². (x 15,000)

Figure 13 (x 15,000)

Figure 14. Section parallel to one of the glide planes. Crystal oriented for double glide. Slip direction in this plane is vertical. (x 15,000).